Research Square

Preprints are preliminary reports that have not undergone peer review.
They should not be considered conclusive, used to inform clinical practice,
or referenced by the media as validated information.

Targeting SYK overcomes acquired resistance to inavolisib in PIK3CA- mutant HER2+ breast cancer

Shengnan Huang
The First Affiliated Hospital, Sun Yat-sen University
Xiaomei Zhang
The First Affiliated Hospital, Sun Yat-sen University
Tiantian Yu
The First Affiliated Hospital, Sun Yat-sen University
Lei Wang
The First Affiliated Hospital, Sun Yat-sen University
Jianping Guo
The First Affiliated Hospital, Sun Yat-sen University
Wei Xie
The First Affiliated Hospital, Sun Yat-sen University
Ying Lin
linying3@mail.sysu.edu.cn

The First Affiliated Hospital, Sun Yat-sen University

Research Article

Keywords: Inavolisib, PIK3CA, SYK, Breast cancer therapy, Drug resistance

Posted Date: November 4th, 2026

DOI: https://doi.org/10.21203/rs.3.rs-10193953/v1

License: This work is licensed under a Creative Commons Attribution 4.0 International License.
Read Full License

Additional Declarations: No competing interests reported.

Abstract

Background

The phosphatidylinositol 3-kinase (PI3K)-protein kinase B (AKT) signaling pathway plays a pivotal role in cancer drug resistance. Thus, targeting this axis provides a vulnerability in cancer therapies, particularly for breast cancer. To this end, inavolisib, a highly selective PI3Kα inhibitor, has been recently approved for clinical use in breast cancer therapies. However, acquired resistance remains a challenge.

Methods

We established the acquired resistance cell lines with *PIK3CA*-mutation to inavolisib in both hormone receptor-positive (HR+) and human epidermal growth factor receptor 2-positive (HER2+) conditions. Subsequently, we screened a library of 1,729 Food and Drug Administration (FDA)-approved compounds using cell viability assays. RNA-seq revealed signaling pathway differences between resistant and parental cells. The synergistic effects of candidate sensitizers with inavolisib were validated using cell viability, colony formation, apoptosis, and wound healing assays. The role of spleen tyrosine kinase (SYK) was assessed by using pharmacological inhibition, CRISPR/Cas9-mediated knockout, and siRNA-mediated knockdown.

Results

Screening of the FDA-approved drug library identified several inhibitors, especially fostamatinib, a well-established SYK inhibitor used for chronic immune thrombocytopenia (ITP), as potent sensitizers in HER2 + inavolisib-resistant cell lines. Further experiments showed that fostamatinib could efficiently sensitize inavolisib-resistant cells to inavolisib treatment by decreasing colony formation and increasing apoptosis. Mechanistically, inavolisib-resistant cells exhibited highly phosphorylated SYK. As a result, *SYK* knockout restored sensitivity to inavolisib and, when combined, synergistically enhanced both this effect and the suppression of cell migration.

Conclusions

These findings together indicate that targeting SYK with fostamatinib overcomes acquired resistance to inavolisib in *PIK3CA*-mutant HER2 + breast cancer cells, supporting further evaluation of this combination in clinical settings.

Background

Human epidermal growth factor receptor 2-positive (HER2+) breast cancer accounts for 15%–20% of all breast cancers and is associated with a poorer prognosis (1). Although anti-HER2 targeted therapies,

including monoclonal antibodies (e.g., trastuzumab, antibody-drug conjugates) and tyrosine kinase inhibitors, have substantially improved outcomes (2), primary and acquired resistance remain major clinical challenges. Oncogenic *PIK3CA* mutations, which occur in approximately 30% of HER2 + breast cancers (3), correlate with lower pathologic complete response rates and resistance to multiple HER2-targeted therapies (4–6). These findings establish *PIK3CA* mutation as a critical driver of treatment resistance in HER2 + breast cancer, highlighting the urgent need to understand and target the underlying signaling mechanisms.

The phosphatidylinositol 3-kinase (PI3K)-protein kinase B (AKT) signaling pathway is the primary downstream effector of *PIK3CA* mutations and plays a pivotal role in tumorigenesis, particularly in breast cancers (7), due to frequent alterations in its key components, including gain-of-function mutations in *PIK3CA* and *AKT*, amplification of *HER2*, or loss-of-function mutations in *PTEN* (8–10). Although this pathway is primarily known for promoting tumor growth, its anti-apoptotic function has garnered increasing attention in the context of cancer therapies, including chemotherapy, radiotherapy, and targeted therapies (11–13). Consequently, the PI3K-AKT axis has been considered a key target for restoring therapeutic efficacy. To this end, substantial efforts have been devoted to developing PI3K and AKT inhibitors for cancer treatment. However, adverse effects have hindered this development. More recently, small-molecule drugs, including the AKT inhibitor capivasertib and the PI3Kα inhibitors alpelisib and inavolisib, have been approved by the Food and Drug Administration (FDA) for breast cancer therapy (14–16), albeit in specific molecular backgrounds. In HER2 + breast cancer, clinical trials evaluating inavolisib in combination with anti-HER2 therapy are currently ongoing (17). Despite these advances, acquired resistance to PI3Kα inhibitors such as inavolisib inevitably emerges in *PIK3CA*-mutant breast cancer, raising the critical question: Can targeting alternative signaling nodes counteract this acquired resistance?

In response to this question, it is critical to understand the mechanisms underlying acquired resistance to PI3Kα inhibitors in *PIK3CA*-mutant breast cancer. Several resistance mechanisms have been identified, including compensatory activation of bypass signaling pathways, disruption of negative feedback loops, and metabolic or tumor microenvironment adaptations (18–22). Unfortunately, current strategies to circumvent these mechanisms have shown limited success. Combinations with mammalian target of rapamycin (mTOR) inhibitors or dual PI3K/mTOR inhibitors are limited by high toxicity and modest efficacy, while targeting a single receptor tyrosine kinase fails to account for the heterogeneity of compensatory signaling (23, 24). Therefore, identifying new therapeutic targets and agents to specifically overcome inavolisib resistance in *PIK3CA*-mutant HER2 + breast cancer represents an urgent and important scientific question.

Spleen tyrosine kinase (SYK) is a non-receptor tyrosine kinase that plays a central role in immune cell signaling (25). The role of SYK in solid tumors remains highly controversial (26). Early studies suggested that SYK functions as a tumor suppressor in breast cancer, and its loss of expression correlates with tumor progression and metastasis (27). However, accumulating evidence has revealed a pro-tumorigenic role of SYK. Aberrant SYK activation or overexpression in multiple solid tumor types is closely linked to

tumor cell migration, invasion, chemoresistance, and the formation of an immunosuppressive tumor microenvironment (28–31). Mechanistically, SYK drives these malignant phenotypes through regulation of multiple cellular processes, including DNA repair signaling, autophagy, cytoskeletal dynamics, and epithelial–mesenchymal plasticity, as well as modulation of the tumor immune microenvironment (28–31). Fostamatinib is an oral SYK inhibitor approved by the FDA for the treatment of immune thrombocytopenia (ITP) (32). Leveraging its favorable safety profile and pharmacokinetic properties, the antitumor potential of fostamatinib in solid tumors is being increasingly explored. Preclinical studies have shown that fostamatinib can remodel the tumor microenvironment, enhance antitumor immune responses, and synergize with chemotherapy or targeted therapy in certain models (26, 33, 34).

Here, we established multiple HER2 + breast cancer cell lines with acquired resistance to inavolisib. Using an FDA-approved drug library, we identified fostamatinib as a compound that synergizes with inavolisib to overcome this resistance. We further demonstrated that fostamatinib suppresses proliferation and migration of resistant cells by targeting SYK, offering a promising combination strategy against inavolisib resistance, particularly in HER2 + breast cancer settings.

Methods

Cell culture and transfection

HEK293T, T47D, T47D-R, MDA-MB-453, and MDA-MB-453-R cells were maintained in DMEM (HyClone) supplemented with 10% fetal bovine serum (FBS, Gibco). HCC1954 and HCC1954-R cells were maintained in RPMI 1640 medium (HyClone) supplemented with 10% FBS. All resistant cell lines (HCC1954-R, MDA-MB-453-R, and T47D-R) were maintained in their respective media supplemented with low-dose inavolisib. Cell transfection, lentiviral production and sgRNA virus packaging and subsequent infection were performed according to the protocols described previously (35). Following viral infection, cells were maintained in the presence of puromycin (1 μg/ml).

Reagents and antibodies

Inavolisib (MCE, HY-101562), Fostamatinib (TargetMol, T6115), Cevidoplenib dimesylate (TargetMol, T39437), Lanraplenib (TargetMol, T11824LL) were used at the indicated concentrations. Anti-phospho-Ser473-AKT antibody (4060), anti-AKT1 antibody (2938), anti-phospho-ERK1/2 antibody (4370), anti-ERK1/2 antibody (4695), anti-phospho-Tyr705-STAT3 (9145S), anti-phospho-STAT3 (12640S) and anti-phospho-Tyr525/526-SYK (2710) were obtained from Cell Signaling Technology. Monoclonal anti-SYK (66721-1-Ig) was obtained from Proteintech. Anti-Vinculin antibody (V4505) was obtained from Merck.

Screening FDA-approved drugs

The FDA-approved drug library, containing 1,729 compounds, was obtained from TargetMol (L4200). Compounds were stored as 10 mM aliquots at -80°C, and were subjected to a maximum of 5 freeze-thaw cycles. HCC1954-R cells (3000 cells/well) and T47D-R cells (4000 cells/well) were seeded in 96-well plates. The optimal cell number was determined to ensure that each was in the growth phase at the end of the assay (~ 70% confluency). Cells were plated one day prior to treatment with each compound (10 μM), vehicle control and inavolisib (80 nM for HCC1954-R, 20 nM for T47D-R) individually or in combination for 48h, and the relative cell viability was measured using Cell Counting Kit-8 (CCK8, DOJINDO) assay. Drug synergy scores were calculated using the SynergyFinder + web application (http://synergyfinderplus.org) (36). Schematic diagrams illustrating the generation of drug-resistant cells and the screening workflow of the FDA-approved drug library were created using Generic Diagramming Platform (https://biogdp.com) (37).

Cell viability assay and colony formation

Cell viability was determined using the CCK8 (DOJINDO) assay according to the manufacturer's instructions. Cells (3000 or 4000 cells/well) were seeded into 96-well plates and treated with increasing concentrations of the indicated agents for 48h. The absorbance was measured at 450 nm after incubation with 10 μl of CCK-8 reagent for 3h at 37℃. For colony formation assay, cells (1000 cells/well) were seeded into 6-well plates and treated with or without indicated agents for 24h. After treatment, cells were cultured for another 14–20 days until visible colonies formed. The colonies were washed twice with PBS and fixed with 10% acetic acid/10% methanol for 20 minutes at room temperature and then stained with crystal violet. After staining, the plate was washed and air-dried, and the colony numbers (> 50 cells) were counted. Quantification of the results was performed with ImageJ software.

Annexin-V/7-Aminoactinomycin D double staining assay

To detect cellular apoptosis, cells treated with the indicated concentration of drugs for 24h, were co-stained with Annexin-V-phycoerythrin (PE) and 7-Aminoactinomycin D (7-AAD) from Annexin V-PE apoptosis detection kit I (BD Biosciences) according to the manufacturer's instructions. Stained cells were monitored with fluorescence-activated cell sorting.

sgRNAs and siRNAs

The lentiviruses for CRISPR/Cas9-based editing of *SYK* were generated by cloning the annealed short guide RNAs (sgRNAs) into BsmBI-digested lenti-CRISPR V2 vector, which encodes both Cas9 and an sgRNA of interest, as previously described (38). The sgRNAs were designed by

CRISPR design tool (crispr.mit.edu) as listed below:

sg-h*SYK*-1 Forward: 5'-CACCG GAAAGAAGTTCGACACGCTC

sg-h*SYK*-1Reverse: 5'-AAAC GAGCGTGTCGAACTTCTTTC C

sg-h*SYK*-2 Forward: 5'-CACCG ATGAGATCGTACATCTCTCT

sg-h*SYK*-2 Reverse: 5'-AAAC AGAGAGATGTACGATCTCAT C

Small interfering RNAs targeting *SYK* transcript were synthesized by Suzhou Genepharma Co., Ltd. (China) and the target sequences were as follows: si-*SYK*-#1 (5'-GCAGATGGTTTGTTAAGAGTT-3') and si-*SYK*-#2 (5'- GCATGAGTGATGGGCTTTATT-3').

RNA-sequencing assay

For RNA-seq, high-quality total RNA was isolated and RNA-seq libraries were prepared using the Optimal Dual-mode mRNA Library Prep Kit (BGI-Shenzhen, China). The libraries were sequenced on the BGI G400/T7/T10 platform (BGI-Shenzhen, China). Raw reads were filtered using SOAPnuke (v1.6.5). Clean reads were mapped to NCBI human genome GRCh38. Raw counts of genes were calculated by RSEM (v1.3.1). Differentially expressed genes were identified by DESeq2 (v1.40.2). KEGG enrichment analysis of differentially expressed genes was performed by Phyper based on a hypergeometric test.

Quantitative Real Time PCR

Total RNA was isolated from the cells using TRIzol Reagent (Invitrogen), and 1 μg of each RNA sample was reverse transcribed to cDNA which was subsequently analyzed by quantitative real time PCR. All reactions were carried out in triplicate. Relative gene expression was calculated using the 2-ΔΔCt method. Housekeeping gene glyceraldehyde-3-phosphate dehydrogenase (*GAPDH*) was used as an internal control to normalize target mRNA expression. Primer sequences used were *SYK* forward (5’-CATACTCCCTATCAGCCAGCCC-3’) and reverse (5’-TGACAATGCAGCTGTAGCCTCT-3’); *GAPDH* forward (5’-CATCAAGAAGGTGGTGAAGCAG-3’) and reverse (5’-CGTCAAAGGTGGAGGAGTGG-3’).

Immunoblotting (IB)

Cells were lysed in EBC buffer (50 mM Tris pH 7.5, 120 mM NaCl, 0.5% NP-40) supplemented with protease inhibitors (#4693132001, Roche) and phosphatase inhibitors (#4906837001, Roche). Whole cell lysates were cleared by centrifugation at 8,000 rpm for 3 min. Protein concentrations were determined using the Pierce™ BCA Protein Assay Kit (23225). Equal amounts of protein were mixed with 5× SDS loading buffer and boiled for 10 min. Equal amounts of whole cell lysates were resolved by SDS-PAGE and immunoblotted with indicated antibodies. All antibodies were used at their recommended dilutions in TBST buffer with 5% bovine serum albumin (BSA) for western blot. Quantification of the immunoblot band intensity was performed with Image J (v1.54p) software.

Wound healing assays

A line was scratched through confluent cultures in six-well plates. After washing with PBS, the cells were cultured in serum-free medium containing the indicated drugs for 24h. The gap was inspected by microscopy over time as the cells migrated into the wounded area.

Quantification and statistical analyses

GraphPad Prism (10.1.2) was used for statistical analysis. For all experiments, data were analyzed by one-way analysis of variance (*ANOVA*) or two-way *ANOVA*. N represents the number of independent experiments. Results were considered significant at $*P < 0.05$, $**P < 0.01$, $***P < 0.001$, and $****P < 0.0001$.

Results

Generation of inavolisib-resistant breast cancer cell lines for FDA drug library screening

Drug repurposing is widely adopted due to its low cost and short development cycle (39). The new PI3Kα inhibitor inavolisib has shown clinical promise in *PIK3CA*-mutant advanced breast cancer. The INAVO120 trial demonstrated significant PFS and OS benefit in hormone receptor-positive (HR+) / human epidermal growth factor receptor 2-negative (HER2-) patients, while the INAVO122 trial is ongoing in HER2 + populations (14, 17). Based on this clinical background, to investigate the potential drug resistance to inavolisib, we established two *PIK3CA*-mutant HER2 + resistant cell lines (HCC1954-R and MDA-MB-453-R) and one *PIK3CA*-mutant HR+/HER2- resistant cell line (T47D-R) by gradually increasing drug concentrations over approximately 4 months (Fig. 1A-C, **Fig. S1A**). These models were used to further screen for drugs that sensitize resistant cells to inavolisib.

Using a library of 1,729 FDA-approved compounds, we performed Cell Counting Kit-8 (CCK8)-based screening assays in HCC1954-R and T47D-R cells to identify compounds that enhance the effect of inavolisib (Fig. 1D, **Fig. S1B**). In HCC1954-R cells, the first-round screen selected compounds with a relative cell viability ratio < 0.5 (combination *vs* inavolisib alone), yielding 170 candidates. The second-round screen applied a ratio < 0.5 (combination *vs* candidate alone) to exclude compounds with excessive single-agent toxicity. Among these, fostamatinib, a well-established SYK inhibitor, was identified as a potential sensitizer to inavolisib in HER2 + breast cancer cells (Fig. 1E). However, after the second-round screening, we did not identify any compound that specifically sensitized T47D-R cells to inavolisib (**Fig. S1B**), indicating that no FDA-approved drug could efficiently enhance inavolisib efficacy in HR+ breast cancer cells. Together, these findings suggest that the oral SYK inhibitor fostamatinib has potential beyond its approved indications in the context of inavolisib resistance. We next focused on the synergistic effect of fostamatinib and inavolisib in *PIK3CA*-mutant HER2 + resistant cells.

Fostamatinib synergizes with inavolisib to overcome acquired resistance in PIK3CA-mutant HER2 + breast cancer cells

To validate the synergy between fostamatinib and inavolisib, we performed CCK8 assays and calculated drug synergy scores as previously reported (36). All four synergy models produced scores above 10, indicating strong synergy between fostamatinib and inavolisib in PIK3CA-mutant HER2^{+} resistant cells (Fig. 2A-B). In contrast, no synergy was observed in the corresponding parental cells or T47D-R cells (Fig. 2C-D, **Fig. S1C**), suggesting subtype- and resistance-specific effects. Colony formation assays showed that the combination of fostamatinib and inavolisib significantly reduced the number and size of colonies in resistant breast cancer cells (Fig. 3A), accompanied by elevated cell apoptosis, as detected by Annexin-V/7-Aminoactinomycin D (7-AAD) double staining assays (Fig. 3B). However, fostamatinib alone did not exhibit significant toxicity in resistant or parental cancer cells across these assays (Fig. 2, Fig. 3). These results demonstrate that fostamatinib synergizes with inavolisib to overcome acquired resistance in *PIK3CA*-mutant HER2 + breast cancer cells by suppressing cell viability, clonogenic capacity, and promoting apoptosis.

Fostamatinib targets SYK to sensitize PIK3CA-mutant HER2 + resistant cells to inavolisib

We performed transcriptomic profiling of HCC1954-R and parental cells to explore the mechanism of inducing drug resistance. Specifically, we observed that ECM-receptor interaction, focal adhesion, MAPK, and PI3K-AKT pathways were upregulated in the resistant cells (Fig. 4A). However, *SYK* mRNA level was downregulated in HCC1954-R (Fig. 4B, 4E). Western blot showed that phosphorylated SYK (p-SYK) level was higher in resistant cells than in parental cells (Fig. 4B), despite reduced total SYK protein, which is consistent with a previous finding that its protein level inversely correlated with its phosphorylation and activation (40). This indicates that SYK is activated through post-translational modification despite transcriptional suppression. In addition, p-ERK levels were elevated in resistant cells **(**Fig. 4B**)**, suggesting MAPK pathway activation. The increase in p-SYK and p-ERK may have maintained p-AKT levels in resistant cells comparable to those in parental cells. After combination treatment, p-SYK and p-ERK levels were markedly reduced (Fig. 4B), which could sensitize cells to cell death.

To determine the function of SYK in resistant cells, we first performed drug synergy experiments with highly selective SYK inhibitors, cevidoplenib and lanraplenib, that have not been clinically approved (41, 42). Both inhibitors also showed synergy with inavolisib in *PIK3CA*-mutant HER2 + resistant cells (Fig. 4C, S1D). We then knocked down *SYK* using different siRNAs (Fig. 4D-E). CCK8 assays showed that *SYK* knockdown reduced the IC50 of resistant cells compared to control cells (Fig. 4F), suggesting that the aberrantly activated SYK is required for maintaining inavolisib resistance. We further generated *SYK* knockout (sg*SYK*) resistant cells using CRISPR/Cas9 (Fig. 4G). CCK8 assays confirmed that *SYK* knockout also sensitized resistant cells to inavolisib, as evidenced by a reduced IC50 (**Fig. S1E**). Colony formation assays showed that sg*SYK* alone decreased the clonogenic capacity of resistant cells, and the combination with inavolisib resulted in a more pronounced suppression, indicating a synergistic effect on long-term cell survival (Fig. 4H). Annexin-V/7-AAD double staining assays showed that sg*SYK* alone or inavolisib alone did not induce significant apoptosis. However, sg*SYK* combined with inavolisib markedly increased apoptosis (Fig. 4I). These results together indicate that SYK maintains the resistant

phenotype by supporting proliferation and suppressing apoptosis. Thus, SYK inhibition, particularly in combination with inavolisib, impairs both short-term cell viability and long-term clonogenic survival.

We next assessed the impact of SYK and PI3Kα inhibition on the migratory capacity of resistant cells using scratch wound healing assays. In sg*SYK* resistant cells, depletion of *SYK* alone resulted in only a partial reduction in migration. However, when combined with inavolisib, a marked suppression of cell migration was observed (Fig. 5A, C). Consistent with this finding, pharmacological inhibition of SYK with fostamatinib alone exerted a modest effect on cell migration, whereas the combination with inavolisib led to a substantially more pronounced inhibition (Fig. 5B, D). Taken together, these results demonstrate that concurrent targeting of SYK and PI3Kα is required to effectively impair the migratory capacity of *PIK3CA*-mutant HER2 + resistant cells.

Discussion

Inavolisib, a highly selective PI3Kα inhibitor with mutant-selective and HER2-dependent p110α degrading properties, has shown clinical benefit in *PIK3CA*-mutant breast cancer. It has now received US FDA approval for the treatment of adult patients with *PIK3CA*-mutant, HR+/HER2- locally advanced or metastatic breast cancer (14). However, acquired resistance remains a major challenge. Here, we screened a library of 1,729 FDA-approved compounds and identified the SYK inhibitor fostamatinib as a potent sensitizer to inavolisib in *PIK3CA*-mutant HER2 + resistant cells. As an oral SYK inhibitor, fostamatinib has already been approved for immune thrombocytopenia with a well-characterized safety profile. We show that fostamatinib, by targeting SYK, exerts synergistic antitumor effects with inavolisib in preclinical resistant tumor models, highlighting its potential for later-line treatment. Together, our findings establish SYK as a key mediator of resistance and provide a preclinical rationale for combining fostamatinib with inavolisib to overcome acquired resistance. However, owing to the limited supply of inavolisib, *in vivo* validation of our models could not be conducted, which is essential for determining the efficacy and safety profile of this combination strategy. Additionally, future studies using patient-derived xenograft (PDX) mouse models bearing *PIK3CA*-mutant HER2$^+$ breast cancer are warranted to further validate the potential of this combination approach.

SYK is canonically recognized as a tumor suppressor in normal mammary epithelium and breast cancer cells, where it stabilizes intercellular adhesion, suppresses EMT and cell motility by phosphorylating the E-cadherin/catenin complex, thereby maintaining epithelial integrity (43–45). However, our data reveal a different picture. In *PIK3CA*-mutant HER2 + resistant breast cancer cells, total SYK protein is reduced, but its phosphorylation at Tyr525/526 is markedly elevated (Fig. 4B). This increase in site-specific phosphorylation indicates enhanced SYK kinase activity, despite lower protein levels. A similar observation was reported by Shinde et al. in TGF-β-induced EMT models (40), suggesting that SYK function may be fundamentally rewired under drug-resistant pressure. However, the key downstream targets of SYK, in particular in response to inavolisib resistance in breast cancer, warrant further investigation.

We propose that hyperactivated SYK contributes to resistance through two mechanisms. First, it may participate in compensatory bypass signaling. SYK is known to function downstream of multiple receptor tyrosine kinases, including EGFR and c-Met, which activate MAPK/ERK and PI3K/AKT pathways (46, 47). This is consistent with MAPK activation and p-AKT maintenance in our resistant cells (Fig. 4B). Second, SYK-mediated changes in cell-matrix adhesion may support cell survival. Transcriptomic profiling revealed upregulation of adhesion pathways in resistant cells, which also exhibited elevated SYK phosphorylation (Fig. 4B). This observation aligns with the known functions of SYK in stabilizing intercellular adhesion and inhibiting cell motility (43). We propose that hyperactivated SYK enhances cell adhesion, thereby promoting cell survival under therapeutic stress in the resistant context. Interestingly, combined treatment with inavolisib synergistically suppressed cell migration, likely due to disruption of this adhesion-mediated survival homeostasis (Fig. 5). Meanwhile, enhanced cell-matrix adhesion has been linked to drug tolerance and resistance in multiple cancer types. In HER2 + breast cancer models, activation of the integrin β1/Src axis was shown to mediate resistance to combined HER2 and PI3K inhibition (48). Similarly, in ovarian cancer, ECM-dependent integrin β1 and FAK signaling promotes chemoresistance (49). We speculate that SYK-mediated adhesion in our model may similarly engage these survival pathways to maintain cell viability under therapeutic stress. However, the mechanisms by which SYK regulates adhesion-dependent survival in resistant cells and by which combined SYK and PI3Kα inhibition synergistically suppresses cell migration remain unclear and warrant further investigation.

In summary, our study identifies SYK as a mediator of acquired resistance to PI3Kα inhibition in *PIK3CA*-mutant HER2 + breast cancer. Targeting SYK with fostamatinib restores sensitivity to inavolisib and suppresses tumor growth. These findings provide a preclinical rationale for combining fostamatinib with inavolisib as a potential later-line treatment strategy.

Conclusions

Our findings demonstrate that hyperactivated SYK mediates acquired resistance to the PI3Kα inhibitor inavolisib in *PIK3CA*-mutant HER2 + breast cancer. Targeting SYK with fostamatinib restores sensitivity to inavolisib and suppresses the migratory capacity of resistant cells. These results provide a preclinical rationale for combining fostamatinib with inavolisib as a potential strategy to overcome acquired resistance in this setting.

Abbreviations

AKT
Protein kinase B
Cas9
CRISPR-associated protein 9
CCK8
Cell Counting Kit-8

CRISPR
Clustered regularly interspaced short palindromic repeats
c
Met: Mesenchymal-epithelial transition factor
ECM
Extracellular matrix
ERK
Extracellular signal-regulated kinase
EGFR
Epidermal growth factor receptor
FAK
Focal adhesion kinase
FDA
Food and Drug Administration
GAPDH
Glyceraldehyde-3-phosphate dehydrogenase
HER2- / HER2+
Human epidermal growth factor receptor 2-negative / Human epidermal growth factor receptor 2-positive
HR / HR+
Hormone receptor / Hormone receptor-positive
ITP
Immune thrombocytopenia
MAPK
Mitogen-activated protein kinase
mTOR
Mammalian target of rapamycin
PI3K / PI3Kα
Phosphatidylinositol 3-kinase / Phosphatidylinositol 3-kinase alpha
PTEN
Phosphatase and tensin homolog
PDX
Patient-derived xenograft
STAT3
Signal transducer and activator of transcription 3
SYK
Spleen tyrosine kinase

Declarations

Ethics approval and consent to participate

Not applicable.

Consent for publication

Not applicable.

Availability of data and materials

The datasets supporting the conclusions of this article are included within the article (and its additional files).

Competing interests

The authors declare no competing interests.

Funding

National Natural Science Foundation of China (No: 82372781)

National Natural Science Foundation of China (No: 82473404)

Guangdong Health Management Association (No: 2025001)

Authors' Contributions

Conception and design: Y.L., W.X., J.G.; Development of methodology: S.H., X.Z., W.X.; Acquisition of data (e.g., provided cells, provided facilities): S.H., X.Z., T.Y., L.W.; Analysis and interpretation of data (e.g., statistical analysis, biostatistics, computational analysis): S.H., X.Z., T.Y., L.W.; Writing the manuscript: S.H., W.X., J.G.; Administrative, technical, or material support (e.g., reporting or organizing data, constructing databases): S.H., X.Z., T.Y., L.W.; Study supervision: Y.L., W.X.. Approved manuscript: all authors.

Acknowledgements

We thank members of the Guo laboratory for critical reading and kind suggestion of the manuscript.

References

1. Loibl S, Gianni L. HER2-positive breast cancer. Lancet. 2017;389(10087):2415–29. 10.1016/S0140-6736(. 16)32417-5 PubMed PMID: 27939064.
2. Avelino ARM, Pulipati S, Jamouss K, Bhardwaj PV. Updates in treatment of HER2-positive metastatic breast cancer. Curr Treat Options Oncol. 2024;25(12):1471–81. 10.1007/s11864-024-01277-2 . PubMed PMID: 39520520.

3. Berns K, Horlings HM, Hennessy BT, Madiredjo M, Hijmans EM, Beelen K, et al. A functional genetic approach identifies the PI3K pathway as a major determinant of trastuzumab resistance in breast cancer. Cancer Cell. 2007;12(4):395–402. 10.1016/j.ccr.2007.08.030 . PubMed PMID: 17936563.
4. Majewski IJ, Nuciforo P, Mittempergher L, Bosma AJ, Eidtmann H, Holmes E, et al. PIK3CA mutations are associated with decreased benefit to neoadjuvant human epidermal growth factor receptor 2-targeted therapies in breast cancer. J Clin Oncol Off J Am Soc Clin Oncol. 2015;33(12):1334–9. .2158 PubMed PMID: 25559818; PubMed Central PMCID: PMC5087318.
5. Rasti AR, Guimaraes-Young A, Datko F, Borges VF, Aisner DL, Shagisultanova E. PIK3CA mutations drive therapeutic resistance in human epidermal growth factor receptor 2-positive breast cancer. JCO Precis Oncol. 2022;6:e2100370. 10.1200/PO.21.00370 . PubMed PMID: 35357905; PubMed Central PMCID: PMC8984255.
6. Loibl S, Majewski I, Guarneri V, Nekljudova V, Holmes E, Bria E, et al. PIK3CA mutations are associated with reduced pathological complete response rates in primary HER2-positive breast cancer: pooled analysis of 967 patients from five prospective trials investigating lapatinib and trastuzumab. Ann Oncol Off J Eur Soc Med Oncol. 2016;27(8):1519–25. 10.1093/annonc/mdw197 . PubMed PMID: 27177864; PubMed Central PMCID: PMC6279074.
7. Mm YH, Gg S, Ks ZJY, Ww C. Targeting PI3K/akt signal transduction for cancer therapy. Signal Transduct Target Ther. 2021;6(1). 10.1038/s41392-021-00828-5 . PubMed PMID: 34916492.
8. Miron A, Varadi M, Carrasco D, Li H, Luongo L, Kim HJ, et al. PIK3CA mutations in in situ and invasive breast carcinomas. Cancer Res. 2010;70(14):5674–8. 10.1158/0008-5472.CAN-08-2660 . PubMed PMID: 20551053; PubMed Central PMCID: PMC2905503.
9. Yan M, Schwaederle M, Arguello D, Millis SZ, Gatalica Z, Kurzrock R. HER2 expression status in diverse cancers: review of results from 37,992 patients. Cancer Metastasis Rev. 2015;34(1):157–64. 10.1007/s10555-015-9552-6 . PubMed PMID: 25712293; PubMed Central PMCID: PMC4368842.
10. Li J, Yen C, Liaw D, Podsypanina K, Bose S, Wang SI, et al. PTEN, a putative protein tyrosine phosphatase gene mutated in human brain, breast, and prostate cancer. Science. 1997;275(5308):1943–7. 10.1126/science.275.5308. .1943 PubMed PMID: 9072974.
11. Rozengurt E, Soares HP, Sinnet-Smith J. Suppression of feedback loops mediated by PI3K/mTOR induces multiple overactivation of compensatory pathways: an unintended consequence leading to drug resistance. Mol Cancer Ther. 2014;13(11):2477–88. 10.1158/1535-7163.MCT-14-0330 . PubMed PMID: 25323681; PubMed Central PMCID: PMC4222988.
12. Lei C, Li S, Fan Y, Hua L, Pan Q, Li Y, et al. LncRNA DUXAP8 induces breast cancer radioresistance by modulating the PI3K/AKT/mTOR pathway and the EZH2-E-cadherin/RHOB pathway. Cancer Biol Ther. 2022;23(1):1–13. PubMed PMID: 36329030; PubMed Central PMCID: PMC9635553.
13. Wang Z, Huang Y, Zhang J. Molecularly targeting the PI3K-akt-mTOR pathway can sensitize cancer cells to radiotherapy and chemotherapy. Cell Mol Biol Lett. 2014;19(2):233–42. 10.2478/s11658-014-0191-7 . PubMed PMID: 24728800; PubMed Central PMCID: PMC6275747.

14. Wedam S, Narayan P, Gittleman H, Cheng J, Bhatnagar V, Sabit H, et al. US food and drug administration approval summary: inavolisib with palbociclib and fulvestrant for endocrine-resistant, PIK3CA-mutated, hormone receptor-positive, human epidermal growth factor receptor 2-negative, locally advanced or metastatic breast cancer. J Clin Oncol Off J Am Soc Clin Oncol. 2025;43(28):3123–31. 10.1200/JCO-25-00663 . PubMed PMID: 40845250.
15. Dilawari A, Buturla J, Osgood C, Gao X, Chen W, Ricks TK, et al. US food and drug administration approval summary: capivasertib with fulvestrant for hormone receptor-positive, human epidermal growth factor receptor 2-negative locally advanced or metastatic breast cancer with PIK3CA/AKT1/PTEN alterations. J Clin Oncol Off J Am Soc Clin Oncol. 2024;42(34):4103–13. 10.1200/JCO.24.00427 . PubMed PMID: 39159418; PubMed Central PMCID: PMC11588547.
16. Narayan P, Prowell TM, Gao JJ, Fernandes LL, Li E, Jiang X, et al. FDA approval summary: alpelisib plus fulvestrant for patients with HR-positive, HER2-negative, PIK3CA-mutated, advanced or metastatic breast cancer. Clin Cancer Res Off J Am Assoc Cancer Res. 2021;27(7):1842–9. 10.1158/1078-0432.CCR-20-3652 . PubMed PMID: 33168657; PubMed Central PMCID: PMC8535764.
17. Swain SM, Barrios CH, Basho RK, Curigliano G, Harbeck N, Huang CS, et al. INAVO122: a phase III study of maintenance inavolisib or placebo + pertuzumab + trastuzumab following induction with pertuzumab + trastuzumab + a taxane in patients (pts) with PIK3CA-mutated, HER2-positive advanced breast cancer (HER2 + aBC). J Clin Oncol. 2024;42(16suppl):TPS1124–1124. 10.1200/JCO.2024.42.16_suppl.TPS1124.
18. Chakrabarty A, Sánchez V, Kuba MG, Rinehart C, Arteaga CL. Feedback upregulation of HER3 (ErbB3) expression and activity attenuates antitumor effect of PI3K inhibitors. Proc Natl Acad Sci U S A. 2012;109(8):2718–23. 10.1073/pnas.1018001108 . PubMed PMID: 21368164; PubMed Central PMCID: PMC3286932.
19. Hopkins BD, Pauli C, Du X, Wang DG, Li X, Wu D, et al. Suppression of insulin feedback enhances the efficacy of PI3K inhibitors. Nature. 2018;560(7719):499–503. 10.1038/s41586-018-0343-4 . PubMed PMID: 30051890; PubMed Central PMCID: PMC6197057.
20. Gremke N, Besong I, Stroh A, Von Wichert L, Witt M, Elmshäuser S, et al. Targeting PI3K inhibitor resistance in breast cancer with metabolic drugs. Signal Transduct Target Ther. 2025;10(1):92–111. 10.1038/s41392-025-02180-4.
21. Kumari N, Wright SC, Witham CM, Monserrat L, Palafox M, Richard JL, et al. USP10/GSK3β-mediated inhibition of PTEN drives resistance to PI3K inhibitors in breast cancer. J Clin Invest. 2025;135(22):e180927. 10.1172/JCI180927 . PubMed PMID: 40991650; PubMed Central PMCID: PMC12618074.
22. Li R, Wang Y, Xie M. Tumor microenvironment and key signaling pathways in breast cancer progression and therapy resistance: a review. Biomol Biomed. 2026;26(9):1461–75. 10.17305/bb.2026.13708 . PubMed PMID: 41757567; PubMed Central PMCID: PMC13170727.

23. Wise-Draper TM, Moorthy G, Salkeni MA, Karim NA, Thomas HE, Mercer CA, et al. A phase ib study of the dual PI3K/mTOR inhibitor dactolisib (BEZ235) combined with everolimus in patients with advanced solid malignancies. Target Oncol. 2017;12(3):323–32. 10.1007/s11523-017-0482-9 . PubMed PMID: 28357727; PubMed Central PMCID: PMC5447332.
24. Anta TA, Shehadat OA, Taneera J, Aleidi SM, Abuhelwa AA, Alzoubi KH, et al. Dual inhibition of PI3K and mTOR in cancer therapy: Mechanisms, clinical potential, and future perspectives. Pharm Pract. 2026;24(1):1–13. 10.18549/PharmPract.2026.1.3337.
25. Mócsai A, Ruland J, Tybulewicz VLJ. The SYK tyrosine kinase: a crucial player in diverse biological functions. Nat Rev Immunol. 2010;10(6):387–402. 10.1038/nri2765 . PubMed PMID: 20467426; PubMed Central PMCID: PMC4782221.
26. Joshi S. New insights into SYK targeting in solid tumors. Trends Pharmacol Sci. 2024;45(10):904–18. 10.1016/j.tips. .2024.08.006 PubMed PMID: 39322438; PubMed Central PMCID: PMC11984332.
27. Coopman PJ, Do MT, Barth M, Bowden ET, Hayes AJ, Basyuk E, et al. The syk tyrosine kinase suppresses malignant growth of human breast cancer cells. Nature. 2000;406(6797):742–7. doi:10.1038/35021086 PubMed PMID: 10963601.
28. Yu Y, Suryo Rahmanto Y, Shen YA, Ardighieri L. Et. A. Spleen tyrosine kinase activity regulates epidermal growth factor receptor signaling pathway in ovarian cancer. EBioMedicine. 2019. 10.1016/j.ebiom.2019.08.055
29. Moncayo G, Grzmil M, Smirnova T, Zmarz P, Huber RM, Hynx D, et al. SYK inhibition blocks proliferation and migration of glioma cells and modifies the tumor microenvironment. Neuro-Oncol. 2018;20(5):621–31. 10.1093/neuonc/noy008 . PubMed PMID: 29401256; PubMed Central PMCID: PMC5892144.
30. Zhou Q, Tu X, Hou X, Yu J, Zhao F, Huang J, et al. Syk-dependent homologous recombination activation promotes cancer resistance to DNA targeted therapy. Drug Resist Updat Rev Comment Antimicrob Anticancer Chemother. 2024;74:101085. 10.1016/j.drup.2024.101085 . PubMed PMID: 38636338; PubMed Central PMCID: PMC11095636.
31. Yu Y, Gaillard S, Phillip JM, Huang TC, Pinto SM, Tessarollo NG, et al. Inhibition of spleen tyrosine kinase potentiates paclitaxel-induced cytotoxicity in ovarian cancer cells by stabilizing microtubules. Cancer Cell. 2015;28(1):82–96. 10.1016/j.ccell.2015.05.009 . PubMed PMID: 26096845; PubMed Central PMCID: PMC5257279.
32. González-López TJ, Bermejo-Vega N, Cardesa-Cabrera R, Martínez-Robles V, Aguilar-Monserrate G, Pérez-Segura G, et al. Fostamatinib effectiveness and safety for immune thrombocytopenia in clinical practice. Blood. 2024;144(6):646–56. 10.1182/blood.2024024250 . PubMed PMID: 38843478.
33. Hu M, Yin R, Deng K, Xu N. Drug repurposing of fostamatinib against cancer via potential cytotoxicity and immune checkpoint regulation. Front Immunol. 2025;16:1602189. 10.3389/fimmu.2025.1602189 . PubMed PMID: 40510356; PubMed Central PMCID: PMC12158979.

34. Mandal J, Jones TN, Liberto JM, Gaillard S, Wang TL, Shih IM. Dual inhibition of SYK and EGFR overcomes chemoresistance by inhibiting CDC6 and blocking DNA replication. Cancer Res. 2024;84(22):3881–93. 10.1158/0008-5472.CAN-24-0769 . PubMed PMID: 39120597.
35. Xie W, Jiang Q, Wu X, Wang L, Gao B, Sun Z, et al. IKBKE phosphorylates and stabilizes snail to promote breast cancer invasion and metastasis. Cell Death Differ. 2022;29(8):1528–40. 10.1038/s41418-022-00940-1.
36. Margue C, Philippidou D, Kozar I, Cesi G, Felten P, Kulms D, et al. Kinase inhibitor library screening identifies synergistic drug combinations effective in sensitive and resistant melanoma cells. J Exp Clin Cancer Res CR. 2019;38:56. 10.1186/s13046-019-1038-x . PubMed PMID: 30728057; PubMed Central PMCID: PMC6364417.
37. L Z SJHL, Y WM. Generic diagramming platform (GDP): a comprehensive database of high-quality biomedical graphics. Nucleic Acids Res. 2025;53(D1). 10.1093/nar/gkae973 . PubMed PMID: 39470721.
38. Jiang Q, Zhang X, Dai X, Han S, Wu X, Wang L, et al. S6K1-mediated phosphorylation of PDK1 impairs AKT kinase activity and oncogenic functions. Nat Commun. 2022;13(1):1548. 10.1038/s41467-022-28910-8 . PubMed PMID: 35318320; PubMed Central PMCID: PMC8941131.
39. Schipper LJ, Zeverijn LJ, Garnett MJ, Voest EE. Can drug repurposing accelerate precision oncology? Cancer Discov. 2022;12(7):1634–41. 10.1158/2159-8290.CD-21-0612 . PubMed PMID: 35642948.
40. Shinde A, Hardy SD, Kim D, Akhand SS, Jolly MK, Wang WH, et al. Spleen tyrosine kinase-mediated autophagy is required for epithelial-mesenchymal plasticity and metastasis in breast cancer. Cancer Res. 2019;79(8):1831–43. 10.1158/0008-5472.CAN-18-2636 . PubMed PMID: 30733195; PubMed Central PMCID: PMC6467765.
41. Cho S, Jang E, Yoon T, Hwang H, Youn J. A novel selective spleen tyrosine kinase inhibitor SKI-O-703 (cevidoplenib) ameliorates lupus nephritis and serum-induced arthritis in murine models. Clin Exp Immunol. 2023;211(1):31–45. 10.1093/cei/uxac. 096 PubMed PMID: 36346114; PubMed Central PMCID: PMC9993459.
42. Blomgren P, Chandrasekhar J, Di Paolo JA, Fung W, Geng G, Ip C, et al. Discovery of lanraplenib (GS-9876): a once-daily spleen tyrosine kinase inhibitor for autoimmune diseases. ACS Med Chem Lett. 2020;11(4):506–13. 10.1021/acsmedchemlett.9b00621 . PubMed PMID: 32292557; PubMed Central PMCID: PMC7153012.
43. Zhang X, Shrikhande U, Alicie BM, Zhou Q, Geahlen RL. Role of the protein tyrosine kinase syk in regulating cell-cell adhesion and motility in breast cancer cells. Mol Cancer Res MCR. 2009;7(5):634–44. 10.1158/1541-7786.MCR-08-0371 . PubMed PMID: 19435818; PubMed Central PMCID: PMC2788757.
44. Kassouf T, Larive RM, Morel A, Urbach S, Bettache N, Marcial Medina MC, et al. The syk kinase promotes mammary epithelial integrity and inhibits breast cancer invasion by stabilizing the E-

cadherin/catenin complex. Cancers. 2019;11(12):1974. 10.3390/cancers11121974 . PubMed PMID: 31817924; PubMed Central PMCID: PMC6966528.

45. Larive RM, Urbach S, Poncet J, Jouin P, Mascré G, Sahuquet A, et al. Phosphoproteomic analysis of syk kinase signaling in human cancer cells reveals its role in cell-cell adhesion. Oncogene. 2009;28(24):2337–47. 10.1038/onc.2009.99 . PubMed PMID: 19421152.
46. Luangdilok S, Box C, Patterson L, Court W, Harrington K, Pitkin L, et al. Syk tyrosine kinase is linked to cell motility and progression in squamous cell carcinomas of the head and neck. Cancer Res. 2007;67(16):7907–16. 10.1158/0008-5472.CAN-07-0331 . PubMed PMID: 17699797.
47. Yu Y, Rahmanto YS, Lee MH, Wu PH, Phillip JM, Huang CH, et al. Inhibition of ovarian tumor cell invasiveness by targeting SYK in tyrosine kinase signaling pathway. Oncogene. 2018;37(28):3778–89. 10.1038/s41388-018-0241-0 . PubMed PMID: 29643476; PubMed Central PMCID: PMC6043408.
48. Hanker AB, Estrada MV, Bianchini G, Moore PD, Zhao J, Cheng F, et al. Extracellular matrix/integrin signaling promotes resistance to combined inhibition of HER2 and PI3K in HER2 + breast cancer. Cancer Res. 2017;77(12):3280–92. 10.1158/0008-5472.CAN-16-2808 . PubMed PMID: 28396358; PubMed Central PMCID: PMC5482178.
49. Pietilä EA, Gonzalez-Molina J, Moyano-Galceran L, Jamalzadeh S, Zhang K, Lehtinen L, et al. Co-evolution of matrisome and adaptive adhesion dynamics drives ovarian cancer chemoresistance. Nat Commun. 2021;12(1):3904. 10.1038/s41467-021-24009-8 . PubMed PMID: 34162871; PubMed Central PMCID: PMC8222388.

Figures

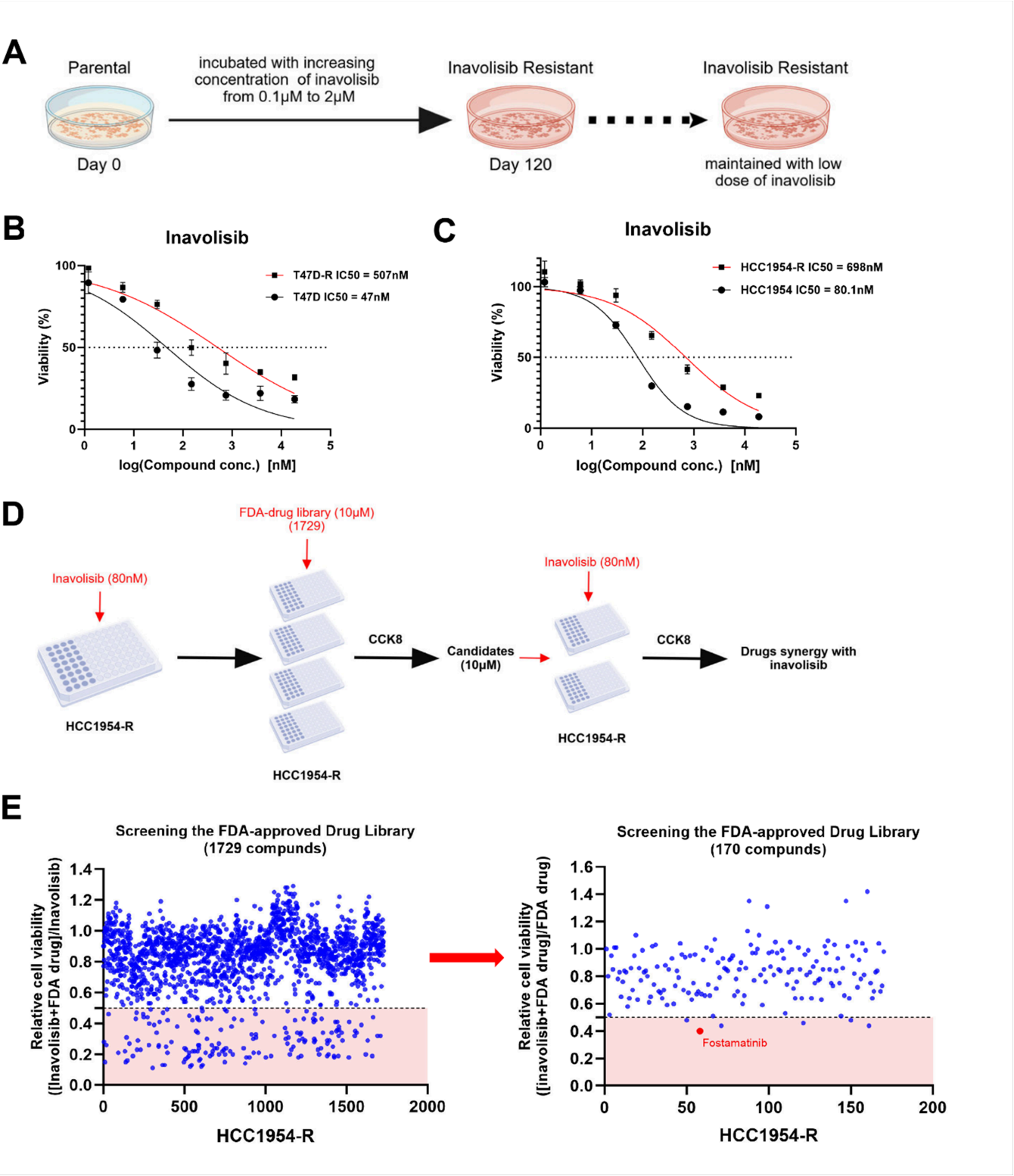


Figure 1

Generation of inavolisib-resistant breast cancer cell lines and FDA drug library screening

(A) Schematic diagram of establishment of inavolisib-resistant breast cancer cells in vitro (created with BioGDP.com).

(B-C) The viability of inavolisib-resistant T47D-R **(B)** /HCC1954-R **(C)** cells and their corresponding parental cells were analyzed by CCK-8 assay. Cells were treated with various concentrations of inavolisib for 48h (n = 3).

(D) Schematic diagram of the workflow for screening the FDA drug library with HCC1954-R cells (created with BioGDP.com).

(E) Results of two-round screening of the FDA-approved drug library (1,729 compounds) in HCC1954-R cells.

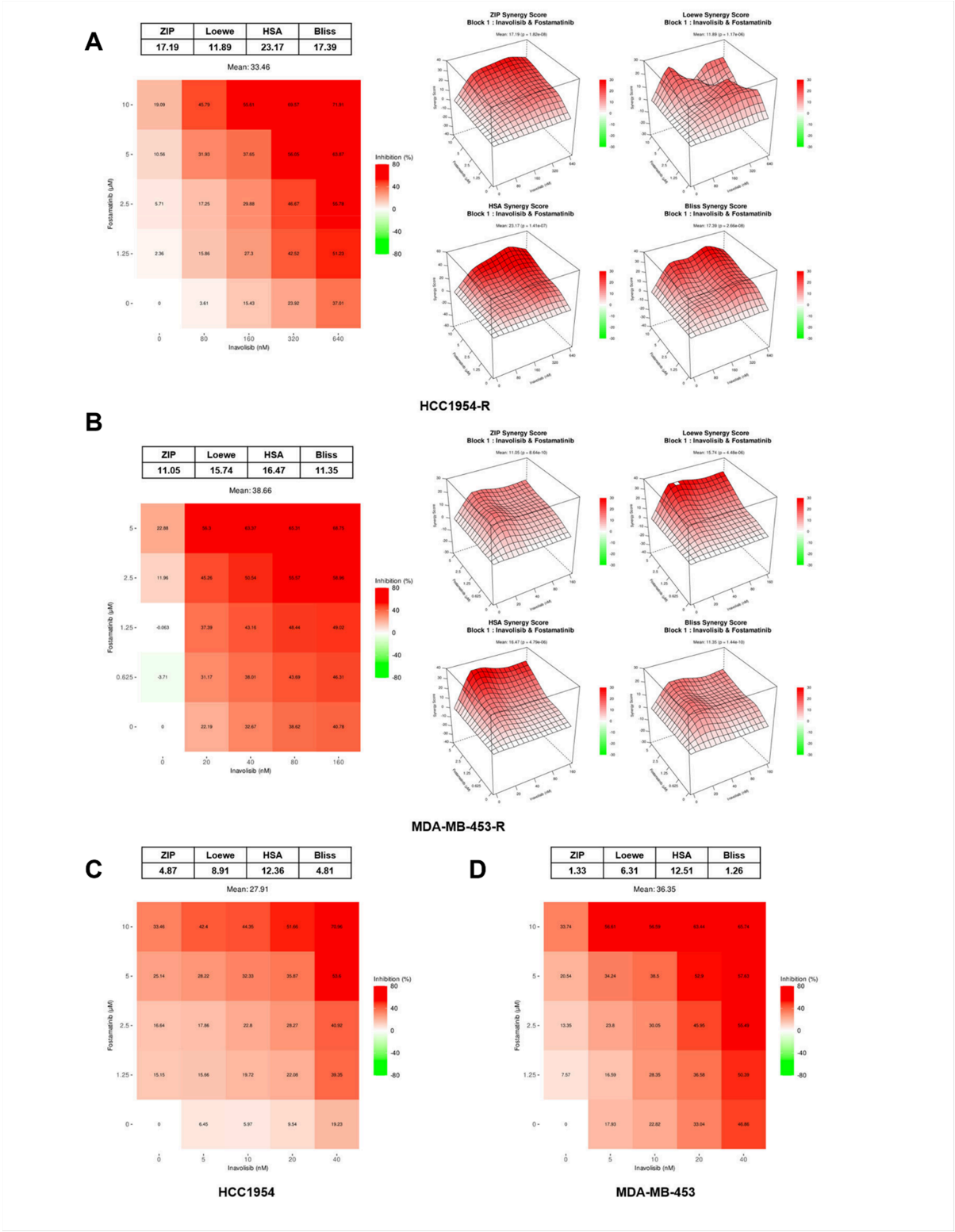


Figure 2

Fostamatinib synergizes with inavolisib in *PIK3CA*-mutant HER2+ resistant cells

(A) HCC1954-R cells were treated with DMSO, inavolisib, fostamatinib, or a combination of inavolisib and fostamatinib as indicated for 48h and then subjected to a CCK-8 assay (lower left panel). The synergy scores (upper left panel) and their 3D representation (right panel) were calculated.

(B) MDA-MB-453-R cells were treated with DMSO, inavolisib, fostamatinib, or a combination of inavolisib and fostamatinib as indicated for 48h and then subjected to a CCK-8 assay (lower left panel). The synergy scores (upper left panel) and their 3D representation (right panel) were calculated.

(C) HCC1954 cells were treated with DMSO, inavolisib, fostamatinib, or a combination of inavolisib and fostamatinib as indicated for 48h and then subjected to a CCK-8 assay (lower panel). The synergy scores (upper panel) were calculated.

(D) MDA-MB-453 cells were treated with DMSO, inavolisib, fostamatinib, or a combination of inavolisib and fostamatinib as indicated for 48h and then subjected to a CCK-8 assay (lower panel). The synergy scores (upper panel) were calculated.

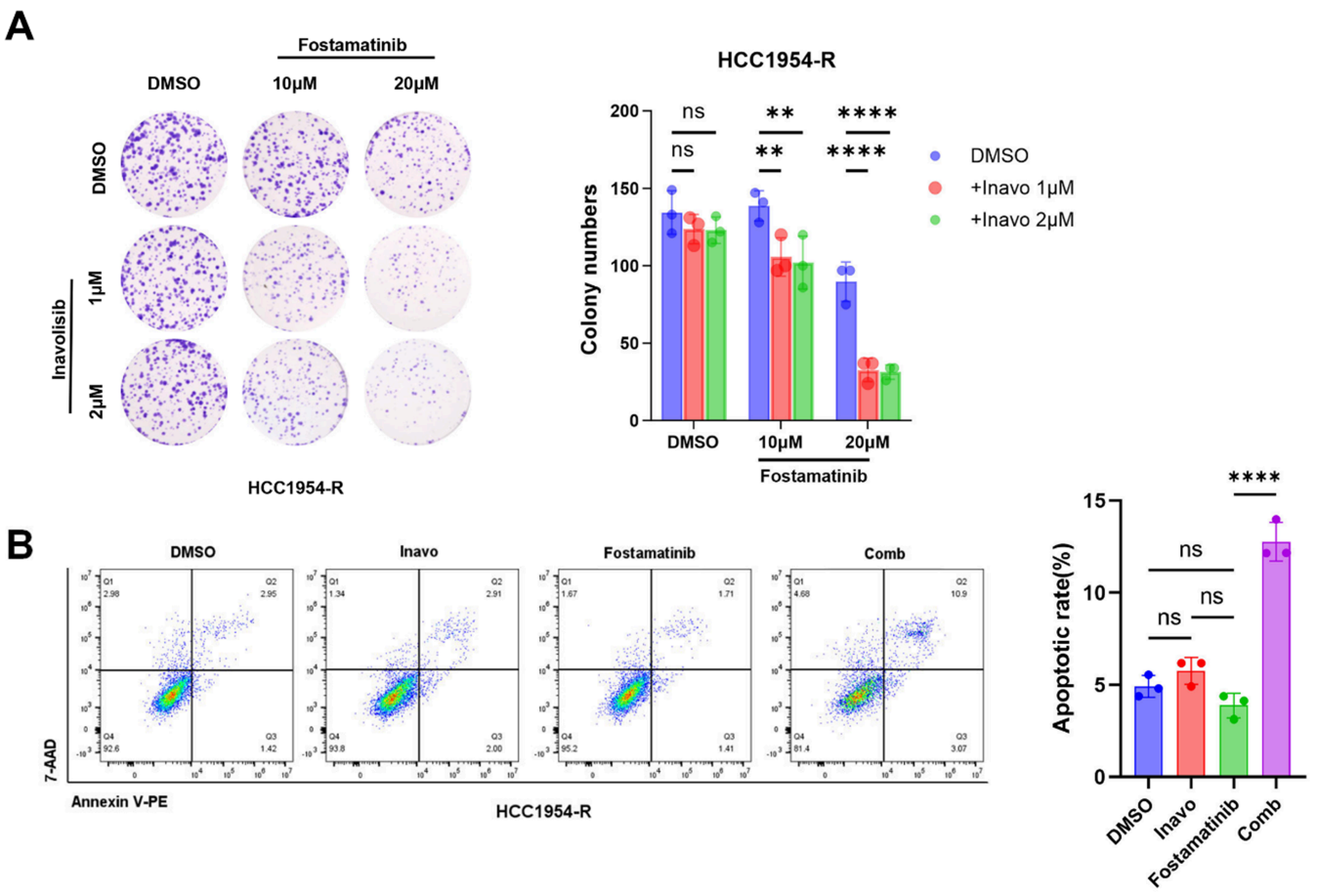


Figure 3

Combination of inavolisib and fostamatinib significantly inhibits *PIK3CA*-mutant HER2+ resistant cells growth

(A) HCC1954-R cells were treated with DMSO, inavolisib, fostamatinib, or a combination of inavolisib and fostamatinib as indicated for colony formation assays (left panel). Colony numbers were quantified,

plotted and analyzed using two-way *ANOVA* (mean ± SD, n = 3) (right panel). ***P* < 0.01, *****P* < 0.0001. ns, no significant.

(B) HCC1954-R cells were treated with DMSO, inavolisib (1 μM), fostamatinib (10 μM), or a combination of inavolisib and fostamatinib for Annexin-V/7-AAD double staining assay (left panel). Apoptotic rate was quantified, plotted and analyzed using one-way *ANOVA* (mean ± SD, n = 3) (right panel). *****P* < 0.0001. ns, no significant.

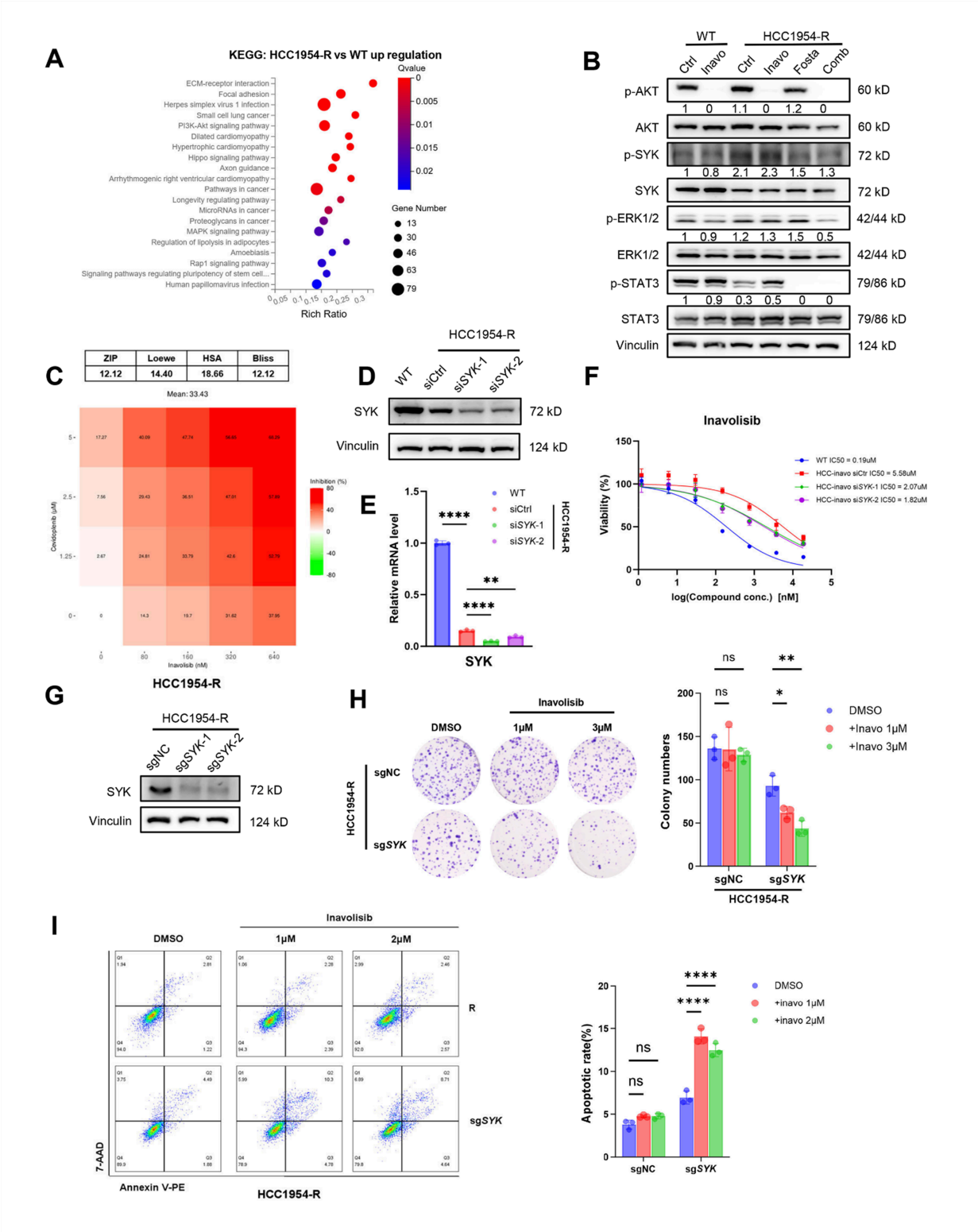


Figure 4

Fostamatinib targets SYK to sensitize *PIK3CA*-mutant HER2+ resistant cells to inavolisib

(A) HCC1954-R cells and HCC1954 cells were harvested, and the mRNAs were extracted for RNA-seq. The results were subjected to KEGG pathway enrichment analysis.

(B) HCC1954 cells were treated with DMSO or inavolisib (0.5 μM) for 20h. HCC1954-R cells were treated with DMSO, inavolisib (0.5 μM), fostamatinib (5 μM), or a combination of inavolisib and fostamatinib for the same duration. All cells were subjected to IB. The relative phosphorylation levels of different groups were represented by the ratio of the phosphorylated protein to its corresponding total protein.

(C) HCC1954-R cells were treated with DMSO, inavolisib, cevidoplenib dimesylate, or a combination of inavolisib and cevidoplenib dimesylate as indicated for 48h and then subjected to a CCK-8 assay (lower panel). The synergy scores (upper panel) were calculated.

(D-E) HCC1954 cells (untreated control) and HCC1954-R cells transfected with control siRNA (siCtrl) or si*SYK* were subjected to IB **(D)** and qPCR **(E)** to confirm *SYK* knockdown. Data were quantified, plotted and analyzed using one-way *ANOVA* (mean ± SD, n = 3). ****P*< 0.01, *****P* < 0.0001. ns, no significant.

(F) The viability of HCC1954-R cells transfected with si*SYK* or siCtrl (from Fig. 4D-E) and HCC1954 cells were analyzed by CCK-8 assay. Cells were treated with various concentrations of inavolisib for 48h (n = 3).

(G-I) HCC1954-R cells were infected with lentivirus ofcontrol sgRNA (sgNC) or sg*SYK*, and *SYK* knockout was confirmed by IB **(G)**. The resulting cells were then subjected to colony formation assay **(H, left panel)** and Annexin-V/7-AAD double staining assay **(I, left panel)**. Colony numbers and apoptotic rates were quantified, plotted and analyzed by two-way *ANOVA* (mean ± SD, n = 3; right panels of H and I). *P < 0.05, **P < 0.01, ****P < 0.0001; ns, not significant.

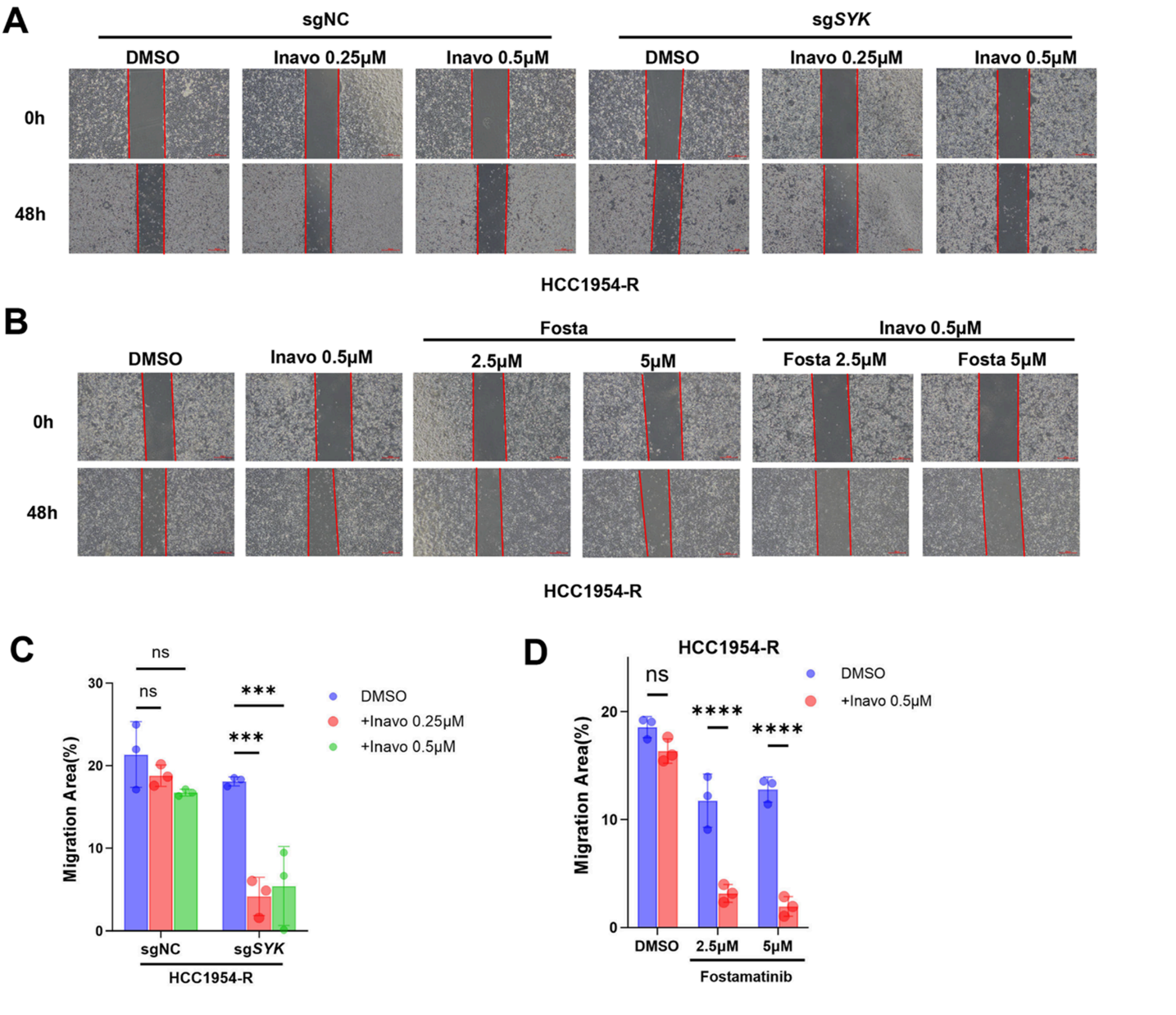


Figure 5

Targeting SYK and PI3Kα synergistically impairs cell motility in *PIK3CA*-mutant HER2+ resistant cells

(A, C) HCC1954-R cells infected with lentivirus of sgNC or sg*SYK* (from Fig. 4G) were treated with inavolisib as indicated for 24h and subjected to wound healing assays**(A)**. Data are presented as the mean ± SD (two-way *ANOVA*) **(C)**. ***P < 0.001, ns, not significant.

(B, D) HCC1954-R cells were treated with DMSO, inavolisib, fostamatinib, or a combination of inavolisib and fostamatinib as indicated for 24h, and subjected to wound healing assays **(C)**. Data are presented as the mean ± SD (two-way *ANOVA*) **(D)**. ****P < 0.0001, ns, not significant.

Supplementary Files

This is a list of supplementary files associated with this preprint. Click to download.

- Additionalfileslegends.docx
- Additionalfile1.pdf
- Additionalfile2.pdf